

See discussions, stats, and author profiles for this publication at: <https://www.researchgate.net/publication/231389204>

Molecule Simulation for the Secondary Reactions of Fluid Catalytic Cracking Gasoline by the Method of Structure Oriented Lumping Combined with Monte Carlo

ARTICLE in INDUSTRIAL & ENGINEERING CHEMISTRY RESEARCH · JUNE 2008

Impact Factor: 2.59 · DOI: 10.1021/ie800023x

CITATIONS

7

READS

13

5 AUTHORS, INCLUDING:



Xiaowei Zhou

Northwestern University

12 PUBLICATIONS 67 CITATIONS

SEE PROFILE

Molecule Simulation for the Secondary Reactions of Fluid Catalytic Cracking Gasoline by the Method of Structure Oriented Lumping Combined with Monte Carlo

Bolun Yang,* Xiaowei Zhou, Chun Chen, Jun Yuan, and Longyan Wang

Department of Chemical Engineering, State Key Laboratory of Multiphase flow in Power Engineering, Xi'an Jiaotong University, Xi'an, 710049, P.R. China

To overcome the drawback of the traditional lumping method, a new method constructed from structure oriented lumping (SOL) combined with Monte Carlo (MC) to simulate the secondary reactions process of fluid catalytic cracking (FCC) gasoline was developed. The SOL method was applied to represent the feedstocks and products configuration framework; then, more than 60 item reaction rules were established to produce all the reaction networks for the secondary reactions of FCC gasoline. By integral calculating each molecule reaction probability using the MC method, the product distribution thus can be obtained. Three samples of catalytic cracking gasoline, taken from the industrial FCC units of China have been used as feedstock of the simulation to check the validity of the proposed method. Some integral properties, such as average molecular weight, element compositions, and hydrocarbon compositions were predicted. The yield of upgraded gasoline, dry gas, liquefied petroleum gas (LPG), light cycle oil (LCO), heavy oil, coke, and olefin changes with extent of reaction were also simulated with this method and the predicted results agreed well with the experimental data.

1. Introduction

The fluid catalytic cracking (FCC) process of heavy hydrocarbons on zeolite catalysts will produce gasoline, diesel, liquefied petroleum gas (LPG), coke, and dry gas by the reactions named primary reactions of oil, such as direct cracking, dehydrogenation, and condensation. However, the gasoline obtained from primary reactions is of low quality with higher olefin and sulfur and it cannot meet the new requirements of the refinery processes. Following these primary reactions, gasoline passes through another riser reactor to undergo a series of secondary reactions, such as cracking, hydrogen transfer, isomerization, aromatization, alkylation, condensation, etc., to obtain a clean gasoline with low olefins and high octane rate. Many catalyst companies have developed several technologies to produce low olefin gasoline and/or to raise propylene yields from FCC units by the use of the secondary reactions of FCC gasoline, in order to comply with increased attention to the olefin issue in FCC process today.^{1,2}

Though the gasoline secondary reaction is not as complex as the primary catalytic cracking process, it still contains hundreds of components and thousands of reactions. Simulation of the feedstock and development of a kinetic model for such complex system are challenging problems because of the lack of fundamental information about feedstock structure and reaction pathways. Traditionally, to simplify the representation of composition and reactions, a technique called lumping^{3–6} has been used to model these complex reaction systems. In lumping models, the many individual chemical species present in the system are grouped into compound classes called kinetic lumps, either from the point of boiling range (i.e., carbon number)^{3,4} or molecular characteristics (paraffins, olefins, naphthenes, and aromatics)^{5,6} then the lumping classes are treated as pseudocomponents. Considering both of the boiling range and molecular

characteristics, an eight lump kinetic model has been proposed to describe the gasoline secondary reaction system in our laboratory.^{7,8} The secondary reaction system is divided into dry gas (DG, H₂, and C₁–C₂), liquefied petroleum gas (LPG, C₃–C₄), light cycle oil (LCO, >477 K), coke (CK), and clean gasoline (GL, C₅+ 477 K); the clean gasoline (GL) is divided into paraffin (GP), olefin (GO), naphthene (GN), and aromatic (GA) groups. The model gives a good prediction for the product distribution. However, the actual composition of lumps in terms of molecular components may change with overall conversion of the system and the lumping kinetics method cannot give a detail description for this kind of variation. Furthermore, it is uncertain whether lumped models can be extrapolated to new conditions or new feedstocks.

Molecular kinetic modeling of hydrocarbon mixtures may overcome many of the insufficiencies associated with lumped kinetic modeling. Quann⁹ and Jaffe¹⁰ have developed a procedure called structure oriented lumping (SOL) to describe molecules and hydrocracking of heavy oil fractions with a notation of vectors, which allows a computer program to represent the reaction networks. The chemical transformations are expressed in terms of the change of a typical structure of the molecules by these authors. Martens^{11,12} and Alwahabi¹³ both have reported a model for the hydrocracking of hydrogenated vacuum gas oil based on theoretical and mechanistic considerations. The reaction mechanism is described by a set of single events, each of which can be ascribed a rate equation or a term in a single rate equation. The model considers the reaction rules for the carbenium ion of the secondary and tertiary types. A computer algorithm, which implements the reaction rules via manipulation of Boolean relation matrices representing the reactant and product, as well as the reaction intermediates, is used for generating the reaction networks. However, these molecular modeling requires a detailed information of feedstock structure, rate constants, and reaction pathways that is often unobtainable from a refinery process.

* To whom correspondence should be addressed. Tel.: +86-29-82663189. Fax: +86-29-82668789. E-mail address: blunyang@mail.xjtu.edu.cn.

Table 1. Properties of the Feedstock

item no.	density 293 K d_{20}^{20}	element composition %				hydrocarbon composition %				boiling range K				
		C	H	S	N	P	O	NA	A	IBP	10%	50%	90%	FBP
1	708.8	86.30	13.59	1.034×10^{-3}	2.0×10^{-5}	36.1	35.2	13.7	15.0	312.5	326	353.5	407	439
2	732.4	86.39	13.46	1.427×10^{-3}	9.2×10^{-5}	30.7	41.8	9.4	18.1	310	330.5	370.8	434	459.8
3	741.1	86.45	13.44	0.951×10^{-3}	5.0×10^{-5}	28.2	43.2	9.3	19.3	312	331	372	439	468

Table 2. Reaction Conditions for Secondary Reactions of Three Sample Feedstocks

reaction condition	1	2	3
temperature (K)	873	873	873
vapor residence time (s)	0.89	1.84	1.96
catalyst to oil ratio	13.8	13.2	13.9

Dynamic Monte Carlo (MC) methods¹⁴ have become effective tools for studying processes that fall between the time and length scales investigated by molecular dynamics and continuum mechanics. Neurock et al.¹⁵ have developed a Monte Carlo resid construction technique whereby petroleum molecules are stochastically constructed by random sampling of probability distribution functions. Monte Carlo sampling of the set (one set for each feed) provide a large ensemble of computer molecules whose properties can be compared to experimentally measured values. An optimized set of parameter values for probability distribution function can be obtained by minimizing a weighted objective function that compares the measured and predicted properties. Compared with molecule methods, the MC method has an advantage where it can just use the common analytic data to simulate the process, while it can not give a proper representation for each molecule as molecule method does.

Considering the characteristics of molecule methods and MC methods, in this work, a new method of SOL combined with MC is employed to simulate the system of secondary reactions of FCC gasoline from molecular scale. Using this combined method, the feedstock is simulated and the molecular kinetic model is also successful established. Hence the reliability of this method is verified.

2. Experiment Data

2.1. Materials. Three samples of catalytic cracking gasoline used in this work were taken from the industrial FCC units of China. Their properties are shown in Table 1.

Y zeolite catalyst (named CC-20D, manufactured by Sinopec Changling Catalyst Co. Ltd., China) which was taken from the circulating inventory of a commercial FCC unit was used in the experiments. The content of Al_2O_3 was 45.2 wt %, the surface area was 98 m^2/g , and the apparent bulk density was 840 kg/m^3 .

2.2. Reaction Conditions. The reactions were conducted in a riser reactor. The main reaction conditions are shown in Table 2.

2.3. Analysis of Feeds and Products. Paraffin, olefin, naphthene, and aromatic compositions of feed gasoline fractions were analyzed by a gas chromatographic procedure described by ASTM D-6733-2001. The coke yield was calculated using flue gas volume and the CO_2 content was analyzed by an infrared analyzer. The gaseous products were analyzed by a HP 6890 multidimension gas chromatography with four valves, two thermal conductivity detectors (TCDs), and five packed columns. The TBP distillation method was used to cut the liquid product into gasoline fractions (C_5^+ 477 K) and light cycle oil fractions ($\text{LCO} > 477 \text{ K}$) that is produced from polymerization of GO, GA, and GN fractions in feed gasoline.

3. Simulation Process. 3.1. Feedstock Simulation. On the basis of the concept of the structure oriented lumping (SOL) approach, the feedstock was represented by a two dimensional matrix **D** in which each row represents a molecule and the row number is the number representing molecules. To create each molecule vector represented by SOL, the random sampling of the Monte Carlo (MC) method was used and provides a large ensemble of calculated molecules whose properties can be compared with experimental measured value.

The construction of a set of representation molecule is accomplished by rigorous assembly of different structural features or increments. The essential idea is to break a molecular type (e.g., PONA) into the most basic structural increments. A structural increment is a specific combination or configuration of C, H, S, and N atoms, often existing in gasoline feedstock. The molecular structure vector **Z** and stoichiometric matrix **G** are defined in Table 3. As shown in Table 3, the increments consist of three types of aromatic rings (A6, A4, A2), six types of naphthenic rings (N6–N1), a methylene $-\text{CH}_2-$ group (R), bridging between rings (A–A), hydrogen deficiency (IH), degree of branching (br), ring substitutions (me), and heteroatom structures containing S and N; it contains a total of 19 types of increments.⁹

Molecular elemental stoichiometry and molecular weight are easily computed from the contributions of the increment's elemental stoichiometry. The overall C, H, S, and N content of any molecule are simply the product of the **G** matrix and its structure vector **Z**:

$$\text{C, H, S, N content} = \mathbf{G} \times \mathbf{Z} \quad (1)$$

The average molecular weight also can be calculated from the C, H, S and N content.

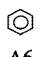

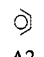
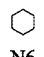

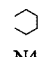
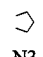
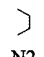
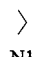
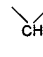
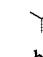
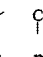
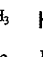
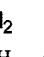

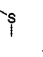

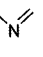
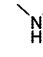
Considering that the feedstock of secondary reactions contains large number of molecules, each molecule can be represented in random sampling method; therefore the probability sampling of the Monte Carlo (MC) method could be applied to produce each molecule. In practice, this amounts to constructing a molecular representation that closely matches analytical measurements and are easily applied to a set of molecules.

The integral properties of feedstock, for example average molecular weight, element compositions, and hydrocarbon compositions, are taken as the average properties of large amount molecules. Thus, the relative errors of the feedstock properties between experiment and calculated results must accord to the normal distribution. The following function is the objective function *F* in the feedstock simulation process.

$$F = \left(\frac{M_e - M_c}{M_e} \right)^2 + \left(\frac{C_e - C_c}{C_e} \right)^2 + \left(\frac{H_e - H_c}{H_e} \right)^2 + \left(\frac{S_e - S_c}{S_e} \right)^2 + \left(\frac{N_e - N_c}{N_e} \right)^2 + \left(\frac{P_e - P_c}{P_e} \right)^2 + \left(\frac{O_e - O_c}{O_e} \right)^2 + \left(\frac{NA_e - NA_c}{NA_e} \right)^2 + \left(\frac{A_e - A_c}{A_e} \right)^2 \quad (2)$$

Where, e and c represent experiment value and calculated value, respectively.

Table 3. Structure Vector Z and Stoichiometric Matrix G of the SOL Approach

Z																			
	A6	A4	A2	N6	N5	N4	N3	N2	N1	R	br	me	IH	AA	NS	RS	AN	NN	RN
G	C	6	4	2	6	5	4	3	2	1	1	0	0	0	0	0	-1	0	0
	H	6	2	0	12	10	6	4	2	0	2	0	0	2	-2	-2	0	-1	-1
	S	0	0	0	0	0	0	0	0	0	0	0	0	0	1	1	0	0	0
	N	0	0	0	0	0	0	0	0	0	0	0	0	0	0	0	1	1	1

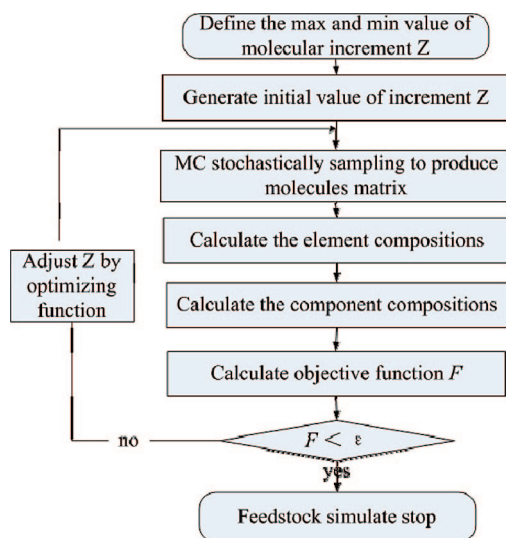


Figure 1. Simulating diagram of feedstock.

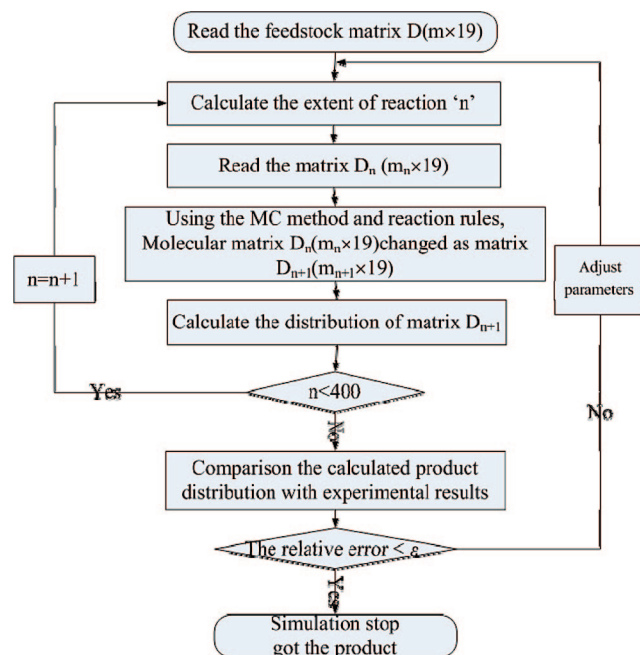


Figure 2. Reaction simulation diagram.

According to the conclusion of chi-square (χ^2) distribution, if X_1, X_2, \dots, X_n are independent of each other and according with normal distribution $N(0,1)$, then the square sum of them must accord with the chi-square (χ^2) distribution.¹⁸

$$\chi^2 = X_1^2 + X_2^2 + \dots + X_n^2 \quad (3)$$

Therefore, the objective function F must be a chi-square (χ^2)

distribution function.

It is known that the probability density function of the χ^2 distribution was shown as follows:¹⁴

$$p(x) = \frac{(x - x_{\min})^{(r/2-1)} \exp\left(-\frac{x - x_{\min}}{2}\right)}{\Gamma(r/2)2^{r/2}} \quad (4)$$

Where, x is the current sample value, x_{\min} is the smallest value of all samples, r is the average value of all samples, and $\Gamma(\alpha)$ is a gamma distribution:

$$\Gamma(\alpha) = \int_0^\infty t^{\alpha-1} \exp(-t) dt \quad (5)$$

In fact, the χ^2 distribution is a special gamma distribution. The gamma distribution probability density function is

$$p(x) = \frac{(x - \gamma)^{(\alpha-1)} \exp\left(-\frac{x - \gamma}{\beta}\right)}{\Gamma(\alpha)\beta^\alpha} \quad (6)$$

For $\gamma = x_{\min}$, $\alpha = r/2$, $\beta = 1/2$, the gamma distribution becomes a χ^2 distribution.

To random sample each increment

$$t = \int_{x_{\min}}^x p(x) dx \quad (7)$$

If $t > RN$ (RN is the uniform distribution between 0 and 1), the value of x is an effective sample; otherwise, the sample is not effective.

Figure 1 shows the simulation diagram for the feedstock. The confine of the molecular increment vector Z should be defined first. This defined method is decided by the feedstock and its structure increments. For example, the feedstock of secondary reaction is gasoline, it means the carbon number will never exceed 12, so the first element A6 (benzene ring) and tenth element R ($-\text{CH}_2-$) of the vector Z shown in Table 3 should not exceed 2 and 12, respectively. The same consideration can be used to define other elements in vector Z , the initial values of vector Z thus will be generated in the defined confine. Then, the molecules matrix can be produced by MC probability sampling. The objective function F is calculated to examine whether the calculated molecules matrix could represent the feedstock. The optimum value of molecular increment vector Z is adjusted by matlab optimizing toolbox.

3.2. Kinetic Model. In order to model the FCC gasoline secondary reactions process, it is necessary to determine which molecules will partake in the secondary reactions and what kind of the reaction pathway should be selected. The first objective will be controlled by reaction rules, and the latter can be decided by the Monte Carlo method.

3.2.1. Reaction Rules. The characteristic feature of the secondary reaction is that all different reactions can be considered as the processes of molecules rearrangements repeat-

Table 4. Predicted Attribute Values of Feedstock

Z	no. 1	no. 2	no. 3	Z	no. 1	no. 2	no. 3
A6	1.5933×10^{-1}	2.0297×10^{-1}	2.0383×10^{-1}	br	3.1512×10^{-1}	2.9358×10^{-1}	3.4488×10^{-1}
A4	4.3623×10^{-3}	9.7521×10^{-3}	1.1007×10^{-2}	me	2.5758×10^{-2}	2.1739×10^{-2}	2.6906×10^{-2}
A2	0	0	0	IH	4.8255×10^{-1}	4.5632×10^{-1}	4.3905×10^{-1}
N6	7.1874×10^{-2}	5.4856×10^{-2}	5.3404×10^{-2}	AA	8.1221×10^{-2}	1.8692×10^{-2}	2.3848×10^{-2}
N5	9.3893×10^{-2}	6.2170×10^{-2}	5.9927×10^{-2}	NS	1.6618×10^{-3}	2.4380×10^{-3}	2.0383×10^{-3}
N4	3.0120×10^{-2}	2.8037×10^{-2}	2.3848×10^{-2}	RS	2.0773×10^{-3}	2.6412×10^{-3}	1.2230×10^{-3}
N3	4.9439×10^{-2}	3.8399×10^{-2}	3.7505×10^{-2}	AN	0	3.0475×10^{-4}	2.0383×10^{-4}
N2	2.7005×10^{-2}	1.9911×10^{-2}	2.0791×10^{-2}	NN	1.6618×10^{-4}	4.0634×10^{-4}	0
N1	0	0	0	RN	0	0	2.0383×10^{-4}
R	5.8031	5.7909	5.8875				

Table 5. Comparison of Experimental Analytical and Predicted Results of No. 1 Feedstock

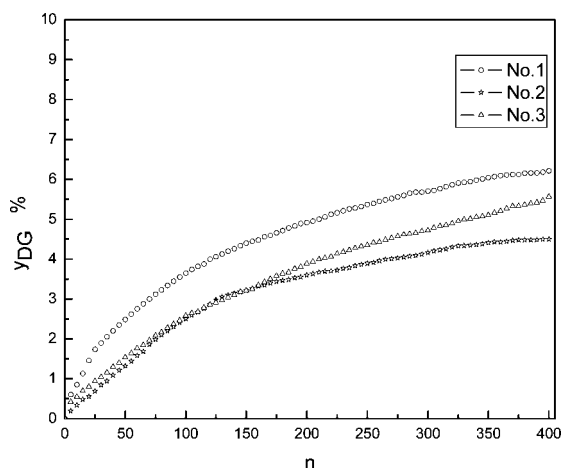
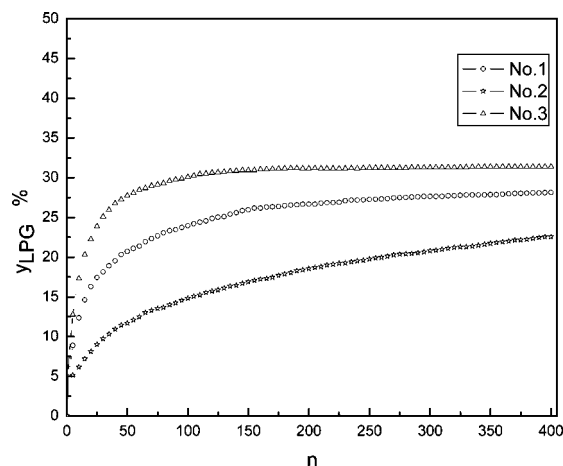
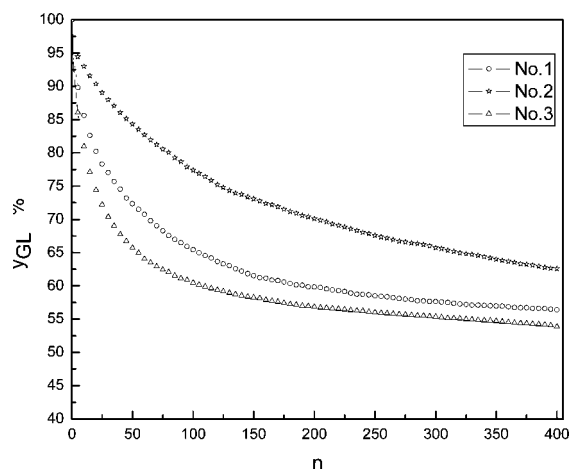
property	experimental data	calculated data	relative error (%)
molecular weight	108.03	111.7	-3.40
C	86.30	85.92	0.44
H	13.59	13.97	-2.80
S	1.034×10^{-3}	1.071×10^{-3}	-3.59
N	2.0×10^{-5}	2.082×10^{-5}	-4.10
P	36.10	33.8	6.37
O	35.20	36.64	-4.09
NA	13.70	13.79	-0.66
A	15.00	15.77	-5.13

Table 6. Comparison of Experimental Analytical and Predicted Results of No. 2 Feedstock

property	experimental data	calculated data	relative error (%)
molecular weight	114.31	110.92	2.97
C	86.39	86.02	0.43
H	13.46	13.82	-2.67
S	1.427×10^{-3}	1.464×10^{-3}	-2.59
N	9.2×10^{-5}	8.998×10^{-5}	2.20
P	30.70	31	-0.98
O	41.80	39.4	5.74
NA	9.40	10.01	-6.49
A	18.10	19.59	-8.23

edly. These particular increments correspond to those structural entities that are rearranged during reactions.

Using a limited set of structural groups to describe thousands of components enables the use of a limited set of reaction rules to establish the complex reaction networks. Each reaction rule consists of a reactant selection rule and a product generation rule. The reactant selection rule first identifies which molecules in the system can undergo a certain structural rearrangement that characterizes a particular type of chemical reaction. Logical constructs are applied to the vectors to determine which components have the increment(s) required for the reaction. The

**Figure 3.** Dry gas yields with the extent of reaction.**Figure 4.** LPG yields with the extent of reaction.**Figure 5.** Gasoline yields with the extent of reaction.

product generation rule is used to convert each reactant's vector to a corresponding product vector. For example, the aromatic saturation rule determines if a molecule has the A4 ring required for the reaction, then converts this ring to an N4(4 carbons) naphthenic ring through a simple mathematical operation. The reactant vector's A4 element is decreased by one and the N4 element is increased by one to create the product vector. Molecules without an A4 ring are not selected for this reaction. Although H2 is a reactant in many reactions, however, it has been considered in the related reactions rule—such as hydrogenation, dehydrogenation, and hydrogen transfer—information on the hydrogen stoichiometry is obtained from the difference in the H content of reactant and product molecules. For this reason, it is not necessary to define a special rule for H2.

The reaction rules contain various reactions in which paraffin, olefin, naphthene, and aromatic hydrocarbon participated, such as thermal cracking, catalytic cracking, hydrogenated saturation,

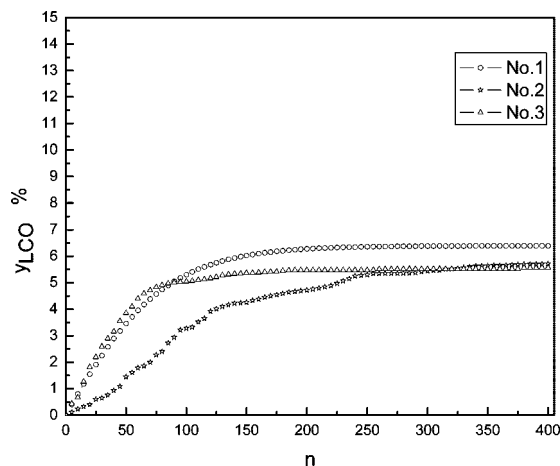


Figure 6. LCO yields with the extent of reaction.

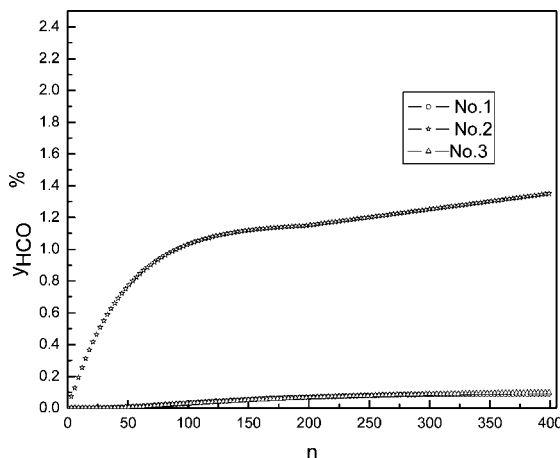


Figure 7. Heavy oil yields with the extent of reaction.

Table 7. Comparison of Experimental Analytical and Predicted Results of No. 3 Feedstock

property	experimental data	calculated data	relative error (%)
molecular weight	114.87	111.79	2.68
C	86.45	86.11	0.39
H	13.44	13.79	-2.60
S	9.51×10^{-4}	9.335×10^{-4}	1.84
N	5.0×10^{-5}	5.105×10^{-5}	-2.10
P	28.20	29.49	-4.57
O	43.20	41.6	3.70
NA	9.30	9.38	-0.86
A	19.30	19.53	-1.19

dehydrogenated cyclization, condensation reaction, polymerization, coke formation, etc. The names for these reaction rules are shown as follows:

Normal Paraffin (4 rules). Catalytic cracking, dehydrogenation and cyclization, thermal cracking, and coke formation.

Iso-paraffin (4 rules). Catalytic cracking, dehydrogenation and cyclization, thermal cracking, and coke formation.

Normal Olefin (5 rules): Catalytic cracking, isomerization, condensation, hydrogenation, thermal cracking, and coke formation.

Iso-olefin (5 rules). Catalytic cracking, isomerization, condensation, hydrogenation, thermal cracking, and coke formation.

Naphthene.

(1) cyclohexane ($R = 0$, 4 rules): ring opening, dehydrogenation, aromatization, and coke formation.

(2) cyclohexane ($R \geq 1$, $R\text{-me} < 3$, 4 rules): ring opening, dehydrogenation, aromatization, and coke formation.

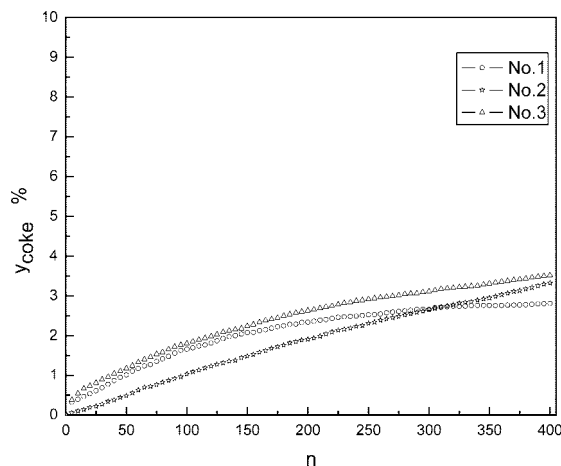


Figure 8. Coke yields with the extent of reaction.

Table 8. Comparison of Predict Product Distribution with Experiment Data for Three Types of Feedstock

product	no. 1		no. 2		no. 3	
	cal value	exp value	cal value	exp value	cal value	exp value
DG wt %	6.21	6.23	4.50	4.48	5.57	5.86
LPG wt %	28.13	28.38	22.56	22.96	31.39	30.82
GL wt %	56.37	56.39	62.57	63.09	53.87	54.40
LCO wt %	6.39	6.26	5.71	5.43	5.56	5.86
HCO wt %	0.09	0.00	1.34	1.24	0.10	0.00
coke wt %	2.81	2.74	3.32	3.76	3.51	3.76

Table 9. Comparison of Predicted Upgraded Gasoline Distribution with Experimental Data for the Three Types of Feedstock

upgraded gasoline composition	no. 1		no. 2		no. 3	
	cal value	exp value	cal value	exp value	cal value	exp value
P wt %	28.26	30.00	28.76	29.70	33.54	34.60
O wt %	18.93	18.70	13.42	13.50	15.55	16.40
N wt %	10.37	9.80	9.47	9.80	12.32	11.20
A wt %	42.44	41.50	48.35	47.00	38.59	37.80

(3) cyclohexane ($R\text{-me} \geq 3$, 2 rules): side chain rupture and coke formation.

(4) cyclopentane ($R = 0$, 2 rules): ring opening and coke formation.

(5) cyclopentane ($R \geq 1$, $R\text{-me} < 3$, 3 rules): ring opening, isomerization, and coke formation.

(6) cyclopentane ($R\text{-me} \geq 3$, 2 rules): side chain rupture and coke formation.

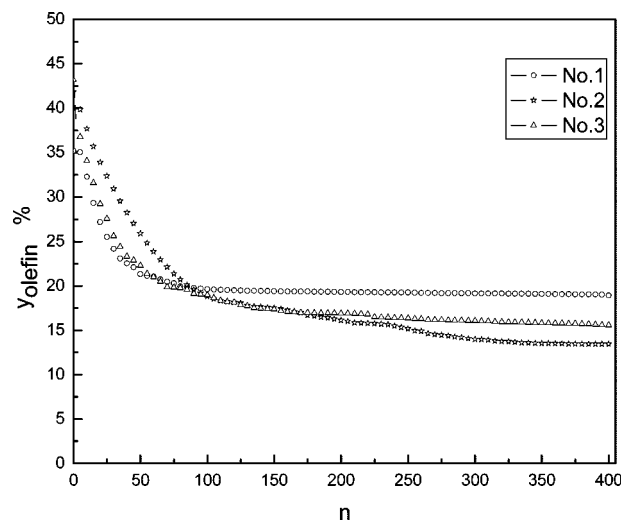


Figure 9. Olefin changes with reaction extent in gasoline.

(7) dicyclo- (N6 + N4, R-me < 2, 3 rules): N4 ring open, N6 ring dehydrogenation, coke formation.

dicyclo- (N6 + N4, R ≥ 2, 2 rules): side chain rupture and coke formation.

(8) dicyclo- (N6 + N3, R = 0, 2 rules): N3 ring opening and coke formation.

dicyclo- (N6 + N3, R ≥ 1, R-me < 3, 3 rules): N3 ring opening, N3 ring isomerization and coke formation.

dicyclo- (N6 + N3, R ≥ 2, 2 rules): side chain rupture and coke formation.

(9) dicyclo- (N5 + N3, R = 0, 2 rules): N3 ring opening and coke formation.

dicyclo- (N5 + N3, R ≥ 1, R-me < 3, 3 rules): N3 ring opening, N3 ring isomerization, and coke formation.

dicyclo- (N5 + N3, R ≥ 2, 2 rules): side chain rupture and coke formation.

Aromatics.

(1) benzene (2 rules): saturation and coke formation.

(2) naphthalene (2 rules): saturation and coke formation.

(3) alkyl aromatics (R ≥ 5, 2 rules): side chain rupture and coke formation.

(4) alkyl aromatics (R ≤ 4, 2 rules): side chain rupture and coke formation.

(5) alkyl aromatics (R-me < 3, 2 rules): condensation and coke formation.

(6) naphthene aromatics (N1 ≥ 1, R = 0, 2 rules): N1 ring opening and coke formation.

(7) naphthene aromatics (N1 ≥ 1, R ≥ 1, 3 rules): N1 ring opening, N1 ring isomerization, and coke formation.

(8) naphthene aromatics (N2 ≥ 1, 3 rules): N2 ring opening, N2 ring dehydrogenation, and aromatization.

(9) naphthene aromatics (N3 ≥ 1, R = 0, 2 rules): N3 ring opening and coke formation.

(10) naphthene aromatics (N3 ≥ 1, R ≥ 1, 3 rules): N3 ring opening, N3 ring isomerization, and coke formation.

(11) naphthene aromatics (N4 ≥ 1, 3 rules): N4 ring opening, N4 ring dehydrogenation, coke formation.

The detailed descriptions for some representative reaction rules were shown in Charts 1–10.

Here, “rand(*a*, *b*)” is the integer uniform distribution between *a* and *b*. When *R*₁ = 3, if *IH*₁ = 1, the products are propane and hexene; otherwise, if *IH*₁ = 0, the products are propylene and hexane. When *R*₁ = 4, if *IH*₁ = 1, the products are butane and pentene; otherwise, if *IH*₁ = 0, the products are butene and pentane.

Chart 1. Paraffin Catalytic Cracking

A

B

C

Reactant selected rule: $R \geq 6$, & $IH = 1$

Product generation rule:

First product : $R_1 = \text{rand}(3, R-3)$, $IH_1 = \text{rand}(0, 1)$

Second product: $R_2 = R - R_1$, $IH_2 = IH - IH_1$

	A6	A4	A2	N6	N5	N4	N3	N2	N1	R	br	me	IH	AA	NS	RS	AN	NN	RN
A	0	0	0	0	0	0	0	0	0	9	0	0	1	0	0	0	0	0	0
B	0	0	0	0	0	0	0	0	0	5	0	0	1	0	0	0	0	0	0
C	0	0	0	0	0	0	0	0	0	4	0	0	0	0	0	0	0	0	0

Chart 2. Paraffin Aromatization

Reactant selected rule: $A6=0, R \geq 6, \& IH=1$

Product generation rule: $A6=1, R=R-6 \& IH=0$

	A6	A4	A2	N6	N5	N4	N3	N2	N1	R	br	me	IH	AA	NS	RS	AN	NN	RN
A	0	0	0	0	0	0	0	0	0	9	0	0	1	0	0	0	0	0	0
B	1	0	0	0	0	0	0	0	0	3	0	0	0	0	0	0	0	0	0

For bond rupture, all the bond strengths of the reactant are treated as equal which means that the probability of rupture at any position is the same. The position of the bond which would rupture is determined by a random function “rand”. Here “rand(*a*, *b*)” is the integer distribution between *a* and *b*. When *R*₁ = 6, the product is 6 carbons + 6 carbon olefins; with *R*₁ = 5, the product is 5 carbons + 7 carbon olefins; when *R*₁ = 4, the product is 4 carbons + 8 carbon olefins; and so on.

3.2.2. Monte Carlo meThod for Monomolecular and Bimolecular Reaction. (1) Monomolecular Reaction. The simulation of the first-order irreversible reaction of A to B averaged a collection of independent Markov chains. A common approximation for the transition probability for a first-order reaction is $P_{AB} = k_{AB}\Delta t + o(\Delta t)$, where $o(\Delta t) \rightarrow 0$ when $\Delta t \rightarrow 0$.¹⁹ In the present approach, for computational motivation, it is useful to allow the fixed Δt to be large, so that the exact solution for P_{AB} could be developed and exploited. The mathematics associated with Markovian processes provide the exact functional form of the A to B reaction probability, P_{AB} , as

$$P_{AB} = 1 - \exp(-k_{AB}\Delta t) \quad (8)$$

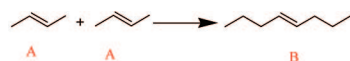
where k_{AB} is the rate constant for the reaction.

The one-step transition probability (*P*) deduced above by matching stochastic and deterministic kinetics will be the basis for the construction of transition probabilities for other simple sequences where such a match is not easily accomplished.

$A \rightarrow B_1$, and $A \rightarrow B_2$. The probability of the disappearance of A by parallel first order paths is determined by using the form of $P_{AB} = 1 - \exp(-k_{AB}\Delta t)$ with its single rate constant (k_{AB}) replaced by the sum $k_{AB1} + k_{AB2}$. Thus, $P = 1 - \exp(-(k_{AB1} + k_{AB2})\Delta t)$. During Monte Carlo simulation, a first-drawn random number (*RN*₁) is compared to *P*, and for *RN*₁ ≤ *P*, a reaction of A occurred, to a yet unspecified product; for *RN*₁ > *P*, A remained intact. When the former condition is met, a second random number (*RN*₂) is drawn to determined the identity of the product. When *RN*₂ ≤ $k_{AB1}/(k_{AB1} + k_{AB2})$, the selectivity or relative probability for the formation of *B*₁, the product is *B*₁; otherwise the product is *B*₂. (2) Bimolecular Reaction. $A + B \rightarrow C$. The transition probability (*P*) of the reaction is obtained from multiplied P_{AC} by P_{BC} , where P_{AC} and P_{BC} are calculated from monomolecular reaction. Thus, the transition probability for each time step is $P = P_{AC} \times P_{BC} = [1 - \exp(-k_{AC}\Delta t)] \times [1 - \exp(-k_{BC}\Delta t)]$.

3.2.3. Rate Constants. From the monomolecular and bimolecular reaction discussion, it is known that the reaction rate

Chart 3. Olefin Condensation

Reactant selected rule: $R \leq 6$, &IH=0Product generation rule: $R=2R$, IH=0

Note: this is a bimolecular reaction.

	A6	A4	A2	N6	N5	N4	N3	N2	N1	R	br	me	IH	AA	NS	RS	AN	NN	RN
A	0	0	0	0	0	0	0	0	0	4	0	0	0	0	0	0	0	0	0
B	0	0	0	0	0	0	0	0	0	8	0	0	0	0	0	0	0	0	0

Chart 4. Olefin Cracking

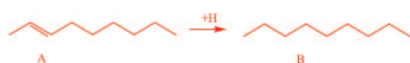
Reactant selected rule: $R \geq 6$ & IH = 0

Product generation rule:

First product: $R_1 = \text{rand}(3, R-3)$, IH1 = 0Second product: $R_2 = R - R_1$, IH2=0.

	A6	A4	A2	N6	N5	N4	N3	N2	N1	R	br	me	IH	AA	NS	RS	AN	NN	RN
A	0	0	0	0	0	0	0	0	0	12	0	0	0	0	0	0	0	0	0
B	0	0	0	0	0	0	0	0	0	7	0	0	0	0	0	0	0	0	0
C	0	0	0	0	0	0	0	0	0	5	0	0	0	0	0	0	0	0	0

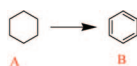
Chart 5. Olefin Hydrogenation

Reactant selected rule: $R \geq 6$, &IH=0Product generation rule: $R=R$, & IH=1

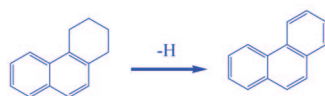
Note: this is a bimolecular reaction.

	A6	A4	A2	N6	N5	N4	N3	N2	N1	R	br	me	IH	AA	NS	RS	AN	NN	RN
A	0	0	0	0	0	0	0	0	0	9	0	0	0	0	0	0	0	0	0
B	0	0	0	0	0	0	0	0	0	9	0	0	1	0	0	0	0	0	0

Chart 6. Naphthene Aromatization

Reactant selected rule: $N_6=1$, $R=0$ & IH=0Product generation rule: $A_6=1$, $N_6=0$, $R=0$ & IH=0

	A6	A4	A2	N6	N5	N4	N3	N2	N1	R	br	me	IH	AA	NS	RS	AN	NN	RN
A	0	0	0	1	0	0	0	0	0	0	0	0	0	0	0	0	0	0	0
B	1	0	0	0	0	0	0	0	0	0	0	0	0	0	0	0	0	0	0



tetrahydrophenanthrene

phenanthrene

Reactant selected rule: $A_6=1$, $A_4=1$, $N_4=1$ Product generation rule: $A_6=1$, $A_4=2$

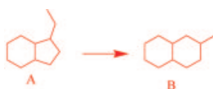
	A6	A4	A2	N6	N5	N4	N3	N2	N1	R	br	me	IH	AA	NS	RS	AN	NN	RN
A	1	1	0	0	0	1	0	0	0	0	0	0	0	0	0	0	0	0	0
B	1	2	0	0	0	0	0	0	0	6	0	0	0	0	0	0	0	0	0

Chart 7. Naphthene Ring Opening

Reactant selected rule: $N_6=1$, $R=0$ & IH=0Product generation rule: $N_6=0$, $R=6$ & IH=0

	A6	A4	A2	N6	N5	N4	N3	N2	N1	R	br	me	IH	AA	NS	RS	AN	NN	RN
A	0	0	0	1	0	0	0	0	0	0	0	0	0	0	0	0	0	0	0
B	0	0	0	0	0	0	0	0	0	6	0	0	0	0	0	0	0	0	0

Chart 8. Naphthene Isomerization

Reactant selected rule: $N_6=1$, $N_3=1$, $R \geq 1$ & IH=0Product generation rule: $N_6=0$, $N_4=1$, $R=R-1$ & IH=0

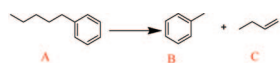
	A6	A4	A2	N6	N5	N4	N3	N2	N1	R	br	me	IH	AA	NS	RS	AN	NN	RN
A	0	0	0	1	0	0	1	0	0	2	0	0	0	0	0	0	0	0	0
B	0	0	0	1	0	1	0	0	0	1	0	0	0	0	0	0	0	0	0

constants are the foundation data to simulate the complex reaction kinetics by the Monte Carlo method. According to the work of Liguras,²⁰ each hydrocarbon in a petroleum mixture consists of a collection of carbon centers and the reaction behavior of hydrocarbon can be described by the reaction behavior of the carbon centers.

For example, if a norm paraffin contains n carbons and its rate constant is r_n , then for other kinds of hydrocarbons which contain the same amount of carbon, its rate constants r'_n can be calculated as follows:

$$r'_n = (X'_n / X_n) \times r_n \quad (9)$$

Chart 9. Aromatic Hydrocarbons Dealkylation



Reactant selected rule: $A_6=1, R \geq 5, IH=0$

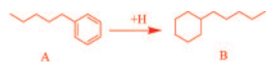
Product generation rule:

First product: $A_6=1, R_1=1, IH_1=0$

Second product: $A_6=0, R_2=R-1, IH_2=0$

	A6	A4	A2	N6	N5	N4	N3	N2	N1	R	br	me	IH	AA	NS	RS	AN	NN	RN
A	1	0	0	0	0	0	0	0	0	5	0	0	0	0	0	0	0	0	0
B	1	0	0	0	0	0	0	0	0	1	0	0	0	0	0	0	0	0	0
C	0	0	0	0	0	0	0	0	0	4	0	0	0	0	0	0	0	0	0

Chart 10. Aromatic Saturation



Reactant selected rule: $A_6=1, R \geq 5, IH=0$

Product generation rule: $A_6=0, N_6=1, R=R \& IH=0$

Note: this is a bimolecular reaction.

	A6	A4	A2	N6	N5	N4	N3	N2	N1	R	br	me	IH	AA	NS	RS	AN	NN	RN
A	1	0	0	0	0	0	0	0	0	5	0	0	0	0	0	0	0	0	0
B	0	0	0	1	0	0	0	0	0	5	0	0	0	0	0	0	0	0	0

where X_n is the relative reactivity of norm paraffin and X_n' is the relative reactivity of the hydrocarbon that needs to be calculated.

In secondary reactions, the reactants mainly include normal paraffin, iso-paraffin, normal olefin, iso-olefin, naphthene, and aromatic hydrocarbons. In this work, normal paraffin and normal olefin (C1–C25) are chosen as the basic model compounds first; the reactions containing these two model compounds mainly include isomerization of norm-olefin, condensation of norm-olefin, hydrogenation of norm-olefin, aromatization and dehydrocyclization of norm-paraffin, thermal cracking of norm-paraffin and norm-olefin, and catalytic cracking of norm-paraffin and norm-olefin. The rate constants for these reactions could be obtained from a literature method.²⁰ Then, using the carbon center method, the rate constants for other reactions, in which iso-paraffin, iso-olefin, naphthene, and aromatic hydrocarbons participated, could be calculated from the rate constants data in which basic model compound participated. Finally, the rate constants in defined temperature are calculated by using the Arrhenius equation.

3.2.4. Product Partition. After simulation of the process of secondary reactions, various molecules will be produced. In order to compare the simulation result with the experimental result, the product molecules must be partitioned. In this work, the product molecules are partitioned as dry gas (DG), liquefied petroleum gas (LPG), upgraded gasoline, light cycle oil (LCO), and coke. During the partition process, dry gas contains H_2 , H_2S , NH_3 , C1, and C2 compounds; LPG contain C1–C3 compounds; gasoline contains the compounds from C5 to C12 (or the compounds whose boiling point was 477 K). C12–C24 compounds are LCO; for the compound which contained more than 24 carbon numbers and if the carbon–hydrogen ratio is smaller than 1, the product is a heavy oil (HCO); otherwise, it is a coke component.

Figure 2 shows the process of feedstock matrix changing as product matrix. There are 400 reaction steps in the process. In each step, there is an “ m_i ” ($i = 0–400$) $\times 19$ matrix. When $i = 0$, the matrix represents the feedstock, and $i = 400$ represents a matrix of the final product. While $i = 1–399$, the matrix represents the middle product.

Take the change of the $m_{40} \times 19$ matrix to the $m_{41} \times 19$ matrix as an example to illustrate this method. First, each molecule which exists in the $m_{40} \times 19$ matrix would be selected, and the category of the selected molecule should be identified (paraffin, olefin, or aromatic). And then, the selected molecule would pass one step reaction (the reaction path was guided by

reaction rules). Finally, the selected molecule changes as the one or two molecules existed in the $m_{41} \times 19$ matrix. After all of the molecules existing in the $m_{40} \times 19$ matrix have finished a one step reaction, then the $m_{40} \times 19$ matrix changes to the $m_{41} \times 19$ matrix. Each feedstock that includes more than a 4000 molecule matrix will undertake same procedure in a series of secondary reactions to become the product. In summary, the 4000 molecule feedstock matrix would undertake 400 matrix step changes in this process.

Besides monomolecular reactions, two kinds of bimolecular reaction which are hydrogenation and condensation may also take place in secondary reaction system; both of them can be expressed as $A + B \rightarrow C$ using one equation. In our simulation process, these reactions are postulated as pseudomonomolecular reaction of $A \rightarrow C$. First, the transition probability is calculated from the bimolecular reaction transition probability which has been described in section 3.2.2. Then, two kinds of parameters for reactant B which are related with hydrogenation and condensation, respectively, are considered in the matrix change to verify the carbon and hydrogen convergence for all bimolecular reactions.

For example, for hydrogenation, the parameter T_i ($i = 1, 2, \dots, 400$) is used as the number of hydrogen change for definite reaction extent. If $T_i > 0$, this means that the redundant hydrogen are produced and the hydrogen content in dry gas will be increased; if $T_i < 0$, this means the hydrogen in dry gas are consumed. The parameter T_i thus is added to the dry gas matrix after matrix change in each reaction extent.

Meanwhile for condensation, parameter R_i ($i = 1, 2, \dots, 400$) is used as the redundant compound between product and reactant. If $R_i > 0$, the reaction is a condensation, and the R_i will be eliminated from the corresponding product matrix after matrix change for definite reaction extent; however, if $R_i = 0$, this means that the reaction is a monomolecular reaction.

4. Results and Discussion

4.1. Predicted Result of Feedstock. Three types feedstock were represented by structure oriented lumping and predicted by the Monte Carlo method. Using this method, more than 4000 molecules were produced to represent each type feedstock. Table 4 shows the three types of simulated feedstock molecular increment values (Z) which are the average values of all simulated molecule increments of each feedstock.

Using the combined method, all the feedstock properties such as average molecular weight, element compositions, and hy-

drocarbon compositions were predicted, except for the gravity and distillation. Tables 5–7 show the comparison of experiment analytical and predicted result for three types of feedstock properties. Most of the results agree well with the experiment feedstock data.

There is a contradiction between the required accuracy of the representation of a feedstock with simulation time for feedstock simulation. The chemical accuracy is a statistical measure of the feedstock's property measurement. The effect of a highly accurate measurement (small standard deviation and objective function F smaller than a defined value) is the requirement that the molecular representation must match that property more closely than a property where there is more uncertainty in the measurement. Through Monte Carlo sampling, each of iteration would construct a large representative sample of molecules. Increasing the sample size can improve the precision of the molecular representation. However, larger sample sizes demand more simulation time. Increasing the sample sizes will increase the represented molecules for reactants but makes the reaction network and the kinetic modeling process more complex. Therefore, the sample size has been limited to not more than 5000 molecules for a practical simulation process.

4.2. Kinetic Model Result. As discussed above, each reactant will pass through series of reactions and construct a Markov chain. Extending the monomolecular reaction Markovian processes to all the secondary reactions and using the reaction rules, the feedstock matrix would change as the product matrix. All reactions are achieved by molecule changes that ensure the material balance. The masses of all elements such as carbon, hydrogen, sulfur and nitrogen are in absolute conservation.

With the feedstock matrix changing with the product matrix process, the feedstock will pass through series of middle processes. In practice, the whole reaction is partitioned to 400 small processes, which means the feedstock changing as product matrix passes through a 400 step process. From expression 8, it is known that Δt is as important as rate constant to control each reactant reaction probability. Here, Δt is expressed as follows:

$$\Delta t = \text{reaction time/steps} \quad (10)$$

The reaction times have been shown in Table 2, so for the three types of feedstock, Δt values are $\Delta t_1 = 0.89/400$, $\Delta t_2 = 1.84/400$, and $\Delta t_3 = 1.96/400$, respectively.

Figures 3–8 show the relationship between mass percent of different products and the extent of reaction. Figure 3 shows that the yield of dry gas (DG) increases until to the completion of reaction. This is because every hydrocarbon can produce dry gas through thermal cracking which could last to the completion of reaction. The same character is also shown in Figure 8 of coke curve; like thermal cracking, the coke formation reaction could also last to completion of the reaction.

In Figure 5, it can be seen that upgraded gasoline yield decreases with the extent of reaction because the feedstock is FCC gasoline in secondary reaction system. While for other products, their yields increase with the extent of reaction.

Figures 4 and 6 show that the yields of petroleum gas (LPG) and light cycle oil (LCO) increase quickly during forepart of reaction process, but the rate of increase then diminishes. This is because, like general the FCC process, most of the reactions take place during the first part of the secondary reaction process.

Table 8 shows the comparison of product distribution between predicted result and experimental data. The predicted results agree well with the experimental data.

Since the olefin content is the main point on which to judge in the quality of gasoline, it is necessary to pay attention to its change in the secondary reaction process.

Figure 9 shows the trend of olefin in gasoline change with the extent of reaction. It can be seen that olefin content is effectively reduced by FCC gasoline secondary reactions. Table 9 shows the comparison of predicted distribution of upgraded gasoline with experimental data. The predicted results agree well with the experimental data.

5. Conclusions

Structure oriented lumping (SOL) combined with the Monte Carlo (MC) method is proposed and applied to the secondary reactions of FCC gasoline.

Three types of gasoline feedstock are represented by SOL, and each molecule is created by MC method; the properties of average molecular weight, the element compositions, and hydrocarbon compositions are predicted. Most of the relative errors between experimental and calculated data for feedstock properties were below 8%. Increasing the sample sizes can improve the precision of the molecular representation; however, larger sample sizes demand more simulation time, having more reactants that make the reaction network more complicated.

A kinetic model is also established for the secondary reactions of FCC gasoline by using the combined method. The model contains more than 60 item reaction rules, and each molecule reaction pathway is guided by the MC method with these reaction rules. The product distribution and their yields were predicted. Since the gasoline qualities, especially olefin content in gasoline, were the most important consideration, the upgraded gasoline distributions and olefin change trend in gasoline were also predicted in the model. There was acceptable agreement with the calculated data and with the experimental data indicating that the combined method is reliable. This method may be a reference for other refinery processes.

Acknowledgment

Financial support for this work from the Key Project of National Natural Science Foundation of China (20436040), National Natural Science Foundation of China (20476084, 20776117), and Specialized Research Fund for the Doctoral Program of Higher Education of China (2007698037) is gratefully acknowledged.

Abbreviations

- b = molecule vector
- d_{15}^{15} , d_{20}^{20} = the relative density at 288 and 293 K, kg/m³
- P = probability density function
- t = sample probability
- X_i = value of i th molecular increment
- A = aromatic hydrocarbon volume content, vol %
- C = carbon content, wt %
- G = stoichiometric matrix
- H = hydrogen content, wt %
- M = molecule weight, g/mol
- N = nitrogen content, wt %
- NA = naphthene volume volume content, vol %
- O = olefin volume volume content, vol %
- P = paraffin volume volume content, vol %
- S = sulfur content, wt %
- T = reaction temperature, K
- $\Gamma(\alpha)$ = gamma distribution
- χ^2 = objective function

Subscripts

e = experimental value

c = calculated value

Literature Cited

- (1) Liu, C. H.; Gao, X. H.; Zhang, Z. D.; et al. Surface modification of zeolite Y and mechanism for reducing naphtha ofefin formation in catalytic cracking reaction. *Appl. Catal. A-Gen.* **2004**, *264*, 225.
- (2) Verstraete, J.; Coupard, V.; Thomazeau, C.; Etienne, P. Study of direct and indirect naphtha recycling to a resid FCC unit for maximum propylene production. *Catal. Today.* **2005**, *106*, 62.
- (3) Weekman, V. W.; Nace, D. M. Kinetic of catalytic cracking selectivity in fixed, moving and fluid bed reactors. *AIChE J.* **1970**, *16*, 397.
- (4) Ancheyta-Juarez, J.; Lopez-Isunza, F. 5-lump kinetic model for gas oil catalytic cracking. *Appl. Catal. A-Gen.* **1999**, *177*, 227.
- (5) Jacob, S. M.; Gross, B.; Voltz, S. E.; Weekman, V. W., Jr. A lumping and reaction scheme for catalytic cracking. *AIChE. J.* **1976**, *22*, 701.
- (6) Deng, X. L.; Sha, Y. X.; Wang, L. Y.; Wang, G. L.; Meng, F. D. Studies on a kinetic model of resid catalytic cracking. *Pet. Pro. Petrochem.* **1994**, *26*, 35.
- (7) Wang, L. Y.; Yang, B. L.; Wang, Z. W. Lumps and kinetics for the secondary reactions in catalytically cracked gasoline. *Chem. Eng. J.* **2005**, *109*, 1.
- (8) Chen, C.; Yang, B. L.; Yuan, J.; Wang, Z. W.; Wang, L. Y. Establishment and solution of eight-lump kinetic model for FCC gasoline secondary reaction using particle swarm optimization. *Fuel* **2007**, *86* (15), 2325–2332.
- (9) Quann, R. J. Modeling the chemistry of complex petroleum mixtures. *Environ. Health Perspect.* **1998**, *106*, 1441.
- (10) Jaffe, S. B. Extension of structure-oriented lumping to vacuum residua. *Ind. Eng. Chem. Res.* **2005**, *44*, 9840.
- (11) Martens, G. G.; Thybaut, J. W.; Marin, G. B. Single-Event Rate Parameters for the Hydrocracking of Cycloalkanes on Pt/US-Y Zeolites. *Ind. Eng. Chem. Res.* **2001**, *40* (8), 1832–1844.
- (12) Martens, G. G.; Marin, G. B. Kinetics for hydrocracking based on structural classes, Model development and application. *AIChE J.* **2001**, *47*, 1607.
- (13) Alwahabi, S. M.; Froment, G. F. Single Event Kinetic Modeling of the Methanol-to-Olefins Process on SAPO-34. *Ind. Eng. Chem. Res.* **2004**, *43*, 5098.
- (14) Dooling, D. J.; Broadbelt, L. J. Generic Monte Carlo Tool for Kinetic Modeling. *Ind. Eng. Chem. Res.* **2001**, *40*, 522.
- (15) Neurock, M.; Libanati, C.; Nigam, A.; Klein, M. T. Monte Carlo simulation of complex reaction systems, molecular structure and reactivity in modeling heavy oils. *Chem. Eng. Sci.* **1990**, *45*, 2083.
- (16) He, L. Z. *Calculation programs in petrochemical process (M)*; China Petrochemical Press: Beijing, 1993; p 14.
- (17) Liang, W. J. *Petroleum Chemistry*; China University of Petro Press: Dongying, 1995; p 98.
- (18) Wang, Z. Q.; Chen, S. S.; *Probability Theory & Mathematical Statistics (M)*; Science Press: Beijing, 1999; p 167.
- (19) McDermott, J. B.; Libanati, C.; Lamarca, C.; Klein, M. T. Quantitative Use of Model Compound Information, Monte Carlo Simulation of the Reactions of Complex Macromolecules. *Ind. Eng. Chem. Res.* **1990**, *29*, 22.
- (20) Liguras, D. K.; Allen, D. T. Structural models for catalytic cracking. 1. model compound reactions. *Ind. Eng. Chem. Res.* **1989**, *28*, 665.

Received for review January 12, 2008

Revised manuscript received April 19, 2008

Accepted May 1, 2008

IE800023X